Iron Loss Calculation for High-Speed Permanent Magnet Machines Considering Rotating Magnetic Field and Thermal Effects

Lin Liu, *Student Member, IEEE*, Youguang Guo, *Senior Member, IEEE*, Gang Lei, *Member, IEEE*, and Jian Guo Zhu, *Senior Member, IEEE*

***Abstract*—Thanks to their many merits such as high power density and fast dynamic response, the high-speed permanent magnet machines (HSPMMs) have attracted increasing industrial and domestic applications. However, the iron loss may become significantly higher at higher operating speed and frequency and it should be carefully considered in the machine design and analysis. In this paper, an advanced iron loss analytical calculation method is applied for HSPMMs in which the influences of rotating magnetic field and thermal field are both considered. A 30 kW, 45000 r/min HSPMM is studied to demonstrate that the proposed model is feasible and advantageous. Analysis results reveal that the predicted iron loss by using the proposed method has satisfactory accuracy with small errors (maximum error of 3.73% and absolute average error of 3.03%) under different operating conditions. The proposed method can also be applied in other electromagnetic devices such as superconducting electrical machines.**

***Index Terms*—High-speed permanent magnet machine, iron loss, rotating magnetic flux density, thermal effect**

I. Introduction

High-speed electric machines, compared with conventional motors, possess irreplaceable advantages and have a broad application prospect in centrifugal compressors, machine tools, flywheels, distributed power generation systems and hybrid electric vehicles. The superiorities mainly include compactness, light-weight, high efficiency, and fast dynamic response [1], [2]. In electrical machines market, induction machines, permanent magnet (PM) synchronous machines and switched reluctance machines are often utilized in high-speed situations [3]. Among these machines, high-speed PM machines (HSPMMs) are considered as favorites due to the relative preponderances as regards high power density, low torque ripple and simple configurations [4], [5].

However, HSPMMs feature high operating speed and frequency, and small thermal dissipation space, implying that the loss density is relatively large and the temperature rise might be high [5]-[8]. Therefore, the accurate computation of power losses is crucial for the HSPMM design to finally guarantee the machine to operate safely and stably.

Stator iron loss, defined as the power lost in the stator magnetic core by the change of magnetic field, accounts for a considerable proportion of total losses, especially in HSPMMs. Meanwhile, due to the complexity of the iron loss mechanism, a lot of work has been carried out for more accurate calculation models in the past decades. The traditional Bertotti separation calculation model was originally utilized for iron loss estimation but it is sometimes no longer applicable when the frequency is high [9]. Recently, finite element analysis (FEA) based on Bertotti model was employed to deal with iron loss estimation considering nonlinear and complex geometric problems [10], [11]. Although the FEA has superiority in iron loss calculation accuracy, more concerns should be given to reduce computational costs. Meanwhile, taking the advantages of high accuracy and computational efficiency, magnetic equivalent circuit (MEC), regarded as a promising analytical method, has been used to estimate the iron loss and analyze the operating performance for various electrical machines [12], [13]. However, the MEC method would have some defects in precisely calculating iron loss since it can just estimate the iron loss resulting from the fundamental waves instead of harmonics [12], [13]. Moreover, high temperature is one of the important characteristics that distinguish high-speed motors from the others, which should also be included in the calculation model.

Therefore, for further improving the iron loss calculation models, in this paper, an advanced iron loss analytical prediction model is applied for the HSPMMs, in which rotating magnetic field and thermal effects are considered. The other parts of this paper is organized as follows. Section II illustrates the principles of the proposed iron loss prediction model. Case studies of a 30 kW, 45000 r/min HSPMM are carried out in Section III, where the iron losses at various operating speeds and temperatures are obtained and compared with the calculation via FEA and the prediction via classical Bertotti separation model. Conclusions of the work with discussions are given in Section IV.

II. Problem Formulation and Iron Loss Model

A. Bertotti separation model

Ideally, the flux density in HSPMM is usually assumed to change sinusoidally, such that the Bertotti separation calculation model, including the hysteresis loss density P_{hL}, average

Manuscript received March 10th, 2021; revised May 12th, 2021; accepted June 26th, 2021. This work was supported in part by Australian Research Council under Discovery Grants DP120104305, DP180100470, and the Foundation of China Scholarship Council under Grant 201906730038. (*Corresponding author: Youguang Guo.*)

L. Liu, Y. Guo, and G. Lei are with School of Electrical and Data Engineering, University of Technology Sydney, NSW 2007, Australia (E-mails: Lin.Liu@student.uts.edu.au; Youguang.Guo-1@uts.edu.au; Gang.Lei@uts.edu.au).

J. Zhu is with School of Electrical and Information Engineering, The University of Sydney, NSW 2006, Australia (E-mail: jianguo.zhu@sydney.edu.au).

Digital Object Identifier will be inserted here upon acceptance.

eddy current loss density P_{eL} and average additional loss density P_{adL}, can be utilized for the calculation of iron loss density in silicon steel sheets. The total iron loss density P_{total} is then predicted as [14]

$$P_{total} = P_{hL} + P_{eL} + P_{adL} \tag{1}$$

and

$$\begin{cases} P_{hL} = K_h \dfrac{\omega_s}{2\pi} B_m^{\alpha} \\ P_{eL} = \dfrac{d^2}{12\eta_{Fe}\rho_{Fe}} \dfrac{1}{T}\int_0^T \left(\dfrac{dB(t)}{dt}\right)^2 dt = K_e \dfrac{1}{T}\int_0^T \left(\dfrac{dB(t)}{dt}\right)^2 dt \\ P_{adL} = \dfrac{\sqrt{\sigma_{Fe} GVS}}{\rho_{Fe}} \dfrac{1}{T}\int_0^T \left|\dfrac{dB(t)}{dt}\right|^{3/2} dt = K_{ad} \dfrac{1}{T}\int_0^T \left|\dfrac{dB(t)}{dt}\right|^{3/2} dt \end{cases} \tag{2}$$

where ω_s is the motor angular frequency, B_m is the magnitude of magnetic flux density, d is the thickness of silicon steel sheet, S is the cross-sectional area of iron core, G=0.1375 is a dimensionless constant, $\sigma_{Fe}=1/\eta_{Fe}$ is the conductivity, V is a parameter characterizing the statistical distribution of the local coercive fields, T is the excitation period, η_{Fe} and ρ_{Fe} are the resistivity and density of core material, respectively, K_h and α are both hysteresis loss empirical coefficients, $K_e = d^2/(12\eta_{Fe}\rho_{Fe})$ is defined as the eddy current loss coefficient, $K_{ad} = \sqrt{\sigma_{Fe} GVS}/\rho_{Fe}$ is set as the additional loss coefficient.

According to the specific research achievements in [14],[15], K_{ad} is very small in high grade steel sheets and the additional loss generally accounts for only a small percentage (less than 1%) of the total iron loss. Hence, for simplifying the iron loss modelling in HSPMMs accounting for the rotating magnetic flux density and thermal effect, this paper ignores the additional loss component. Then, as given in (2), it is convincing that accurate estimations of the magnetic field as well as the coefficients K_h and K_e are the precondition for the calculation of iron loss.

B. Iron loss model considering magnetic harmonics

Caused by the effects of stator slotting and rotor structure, the magnetic field waveforms of PM motors are actually far from sinusoidal. In other words, the magnetic field contains both the fundamental wave and harmonics.

Considering the influences of harmonics and rotating magnetization, based on the harmonic analysis theory, the magnetic flux density waveform at any point in the motor can be decomposed into a series of harmonic components. In this case, the iron loss models can be modified as the sum of all the iron losses due to by the fundamental magnetic field wave as well as all magnetic harmonics [16]. Meanwhile, the elliptical rotating magnetic flux density of the j^{th} harmonic can also be divided into two orthogonal alternating components with the long-axis one marked as $B_{j\max}$ and the short-axis one marked as $B_{j\min}$. As a result, the hysteresis and eddy current loss densities in the elliptical rotating magnetic field can be calculated with $B_{j\max}$ and $B_{j\min}$, as

$$\begin{cases} P_{hL} = \sum_{j=1}^{N} \left[jK_h f (B_{j\max}^{\alpha} + B_{j\min}^{\alpha}) \right] \\ P_{eL} = \sum_{j=1}^{N} [\, j^2 K_e f^2 (B_{j\max}^2 + B_{j\min}^2)] \end{cases} \tag{3}$$

where j is the harmonic order, N is the highest order of harmonics, f is the operating frequency and $f=\omega_s/2\pi$.

As for HSPMMs, the loss characteristics can be affected significantly by the high operating frequency because the skin effect results in uneven distribution of eddy current in the laminations. To consider the frequency effect, the eddy current loss coefficient can be updated as a function of f, as

$$K_e(f) = \frac{3}{D\sqrt{f}} \frac{\sinh(D\sqrt{f}) - \sin(D\sqrt{f})}{\cosh(D\sqrt{f}) - \cos(D\sqrt{f})} \tag{4}$$

where $D=d\sqrt{\pi\mu\sigma_{Fe}}$, and μ is the magnetic permeability.

C. Iron loss model considering thermal effect

HSPMMs usually work under the conditions of high speed and low heat dissipation area, which would greatly promote the temperature rise. The resistance of core materials is sensitive to temperature, by which the iron loss can thus be affected. The material resistance, marked R, is computed based on its dimensions as

$$R = \frac{\eta(T_{\circ C})L}{A_{CS}} \tag{5}$$

where $\eta(T_{\circ C})$ is the material resistivity varying with temperature $T_{\circ C}$, L is the length of current path, and A_{CS} is the cross-section area.

Combining with (2), the empirical coefficients of hysteresis loss and eddy current loss can be re-expressed as

$$\begin{cases} K_h = K_h(T_{\circ C}) \\ K_e = K_e(T_{\circ C}) = \dfrac{d^2}{12\eta_{Fe}(T_{\circ C})\rho_{Fe}} \end{cases} \tag{6}$$

According to the linear relationship theory, the unknown parameter $\eta_{Fe}(T_{\circ C})$ can be calculated by:

$$\eta_{Fe}(T_{\circ C}) = \eta_{Fe}^0 (1 + \mu_T \Delta T_{\circ C}) \tag{7}$$

where η_{Fe}^0 is the equivalent resistivity of materials at 0 ℃, μ_T is the temperature coefficient, which can be obtained by curve fitting the iron loss data measured at different temperatures, and $\Delta T_{\circ C}$ is the temperature variation.

As a result, in combination of (3), (4), (6) and (7), the final iron loss calculation model can be synthesized as

$$\begin{aligned} P_{iron} &= (P_{hL} + P_{eL}) V_s \\ &= \left\{ \begin{array}{l} K_h(T_{\circ C}) \sum_{j=1}^{N} \left[jf (B_{j\max}^{\alpha} + B_{j\min}^{\alpha}) \right] \\ + K_e(f) \dfrac{1}{1 + \mu_T \Delta T_{\circ C}} \bullet \sum_{j=1}^{N} [\, j^2 f^2 (B_{j\max}^2 + B_{j\min}^2)] \end{array} \right\} V_s \end{aligned} \tag{8}$$

where V_s is the volume of the stator core.

III. Calculation and Analysis of Iron Loss

A. Correlation analysis

In this subsection, a 30 kW, 45000 r/min HSPMM is used as an example to showcase the merits of the proposed method. The specifications are given in Table I, while the built 2D FEA is illustrated, as shown in Fig. 1.

The correlations between K_h, K_e and temperature are firstly analyzed to simplify the fitting process of iron loss coefficients. According to the Pearson correlation analysis method [14], a correlation coefficient R_{XY} can be defined as

$$R_{XY}=\frac{\sum_{i=1}^{n}\left(X_i-\bar{\boldsymbol{X}}\right)(Y_i-\bar{\boldsymbol{Y}})}{\sqrt{(X_i-\bar{\boldsymbol{X}})^2(Y_i-\bar{\boldsymbol{Y}})^2}} \tag{9}$$

where $\boldsymbol{X}=\{X_i;\ i=1,\cdots N\}$ is the set of input variables, while $\boldsymbol{Y}=\{Y_i;\ i=1,\cdots N\}$ is the corresponding output variables set, and $\bar{\boldsymbol{X}}$ and $\bar{\boldsymbol{Y}}$ are the means of $\boldsymbol{X}$ and $\boldsymbol{Y}$, respectively. Meanwhile, the closer R_{XY} is to 1, the stronger the correlation between input and output variables.

TABLE I
SPECIFICATIONS OF THE HSPMM

Items	Values	Items	Values
Rate power	30 kW	Stator outer radius	57.5 mm
Poles	2	Stator inner radius	26.5 mm
Slot numbers	24	Rotor outer radius	24.5 mm
Rated current	100 A	Sleeve thickness	3 mm
Rate speed	45000 r/min	Tooth width	5.8 mm
Maximum current	150 A	Air-gap length	2 mm
Maximum speed	67500 r/min	Magnet thickness	14.5 mm
Core material	10JNEX900	Yoke thickness	13.5 mm

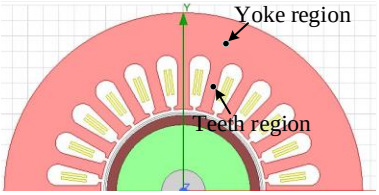

Fig. 1. 2D FEA model of the investigated HSPMM.

Taking advantages of the FEA data, the Pearson correlation coefficients between K_h, K_e and temperature under different working speeds are obtained in Fig. 2. As seen, the average correlation coefficient between hysteresis loss coefficient and temperature is 0.108, while the value for eddy current loss coefficient is 0.889. Thus, the iron loss calculation model expressed by (8) can be updated with (10).

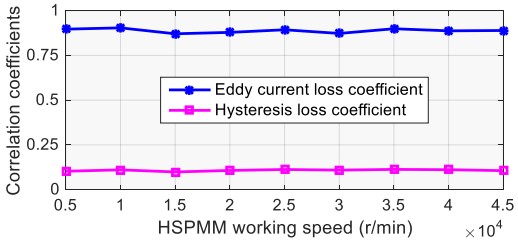

Fig. 2. Correlation between loss coefficients and temperature under different working speeds.

$$P_{iron}=(P_{hL}+P_{eL})\square V_s$$
$$=\left\{\begin{array}{l}K_h\sum_{j=1}^{N}\left[\,jf(B_{j\max}^{\alpha}+B_{j\min}^{\alpha})\right]\\ +K_e(f)\dfrac{1}{1+\mu_T\Delta T_{\circ C}}\bullet\sum_{j=1}^{N}[j^2f^2(B_{j\max}^2+B_{j\min}^2)]\end{array}\right\}\square V_s \tag{10}$$

B. Results analysis

Since the magnetic flux density distribution in the stator core is not uniform, the calculation errors would increase if the average magnetic flux density is utilized. In order to accurately predict the iron loss, the no-load magnetic flux density curves at different parts of HSPMM are obtained, as shown in Fig. 3. The operating speed is set as 30000 r/min. As seen, the magnetic flux density waveform is not ideally sinusoidal due to the harmonics.

Apart from the flux density, the temperature distributions of the stator in HSPMM are also analyzed. For estimating temperature field distribution, it is assumed that no heat exchange happens between stator and rotor. When the experimental HSPMM works at different speeds, the temperatures of different parts in HSPMM are calculated through FEA and given in Table II. As seen, the area in the stator yoke contains more heat and the highest temperature reaches to about 140 ℃.

After fitting the loss coefficients, the Bertotti separation model and the proposed model are both employed to calculate the iron loss of HSPMM taking advantages of the predicted magnetic density waveforms as well as the temperature data given in Table II. The iron loss prediction results are also compared with that obtained via FEA. Figs. 4-6 show the compared results of the HSPMM total iron loss with varying working speeds from 25000 r/min to 60000 r/min under temperature conditions of respectively 40 ℃, 100 ℃ and 150 ℃.

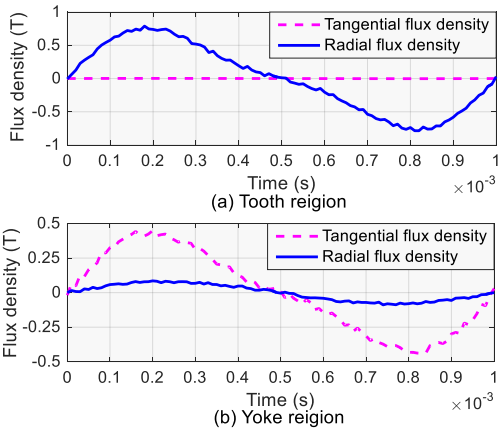

Fig. 3. Magnetic flux densities of HSPMM in different regions.

TABLE II
TEMPERATURES OF HSPMM UNDER DIFFERENT WORKING SPEEDS

Items	30000 r/min	40000 r/min	50000 r/min
Stator yoke	62.3 ℃	103.8 ℃	142.5 ℃
Stator tooth	52.6 ℃	86.5 ℃	120.4 ℃
Coil	59.4 ℃	97.2 ℃	134.6 ℃
Tooth tip	56.2 ℃	89.6 ℃	130.2 ℃
Stator average	57.6 ℃	94.3 ℃	131.9 ℃

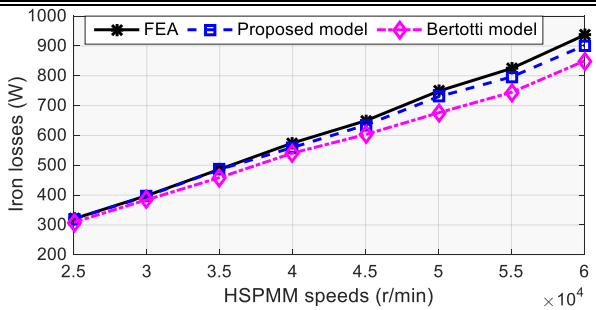

Fig. 4. Comparative results of iron losses with 40 ℃ temperature.

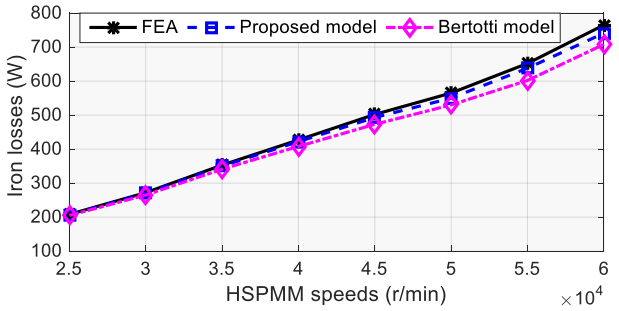

Fig. 5. Comparative results of iron losses with 100 ℃ temperature.

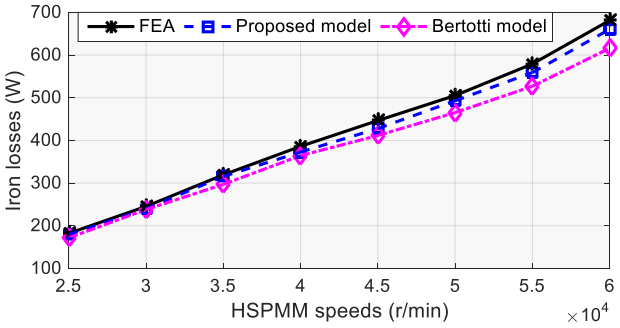

Fig. 6. Comparative results of iron losses with 150 ℃ temperature.

According to the results shown in Figs. 4-6, the related numerical analysis is presented in Table III, where EM_i and EA_i (i=P and B) represent the maximum and absolute average errors of total iron loss obtained by using the proposed model and Bertotti method, respectively. It can be seen that the iron loss decreases by up to 27.28% when the working temperature increases from 40℃ to 150 ℃. Moreover, the iron loss prediction accuracy of the proposed model is pretty high. Under different operating speeds and temperatures, the maximum and absolute average errors of iron loss calculated via the proposed method are respectively less than 3.73% and 3.03% compared with values obtained via FEA, while the maximum and absolute average errors are respectively 9.57% and 7.69% by using Bertotti method.

TABLE III
PREDICTION ERRORS UNDER DIFFERENT TEMPERATURES

Items	40 ℃	100 ℃	150 ℃
EM_P	3.73%	3.14%	3.05%
EA_P	3.03%	2.56%	2.48%
EM_B	9.26%	6.35%	9.57%
EA_B	7.33%	5.25%	7.69%

IV. CONCLUSION

Considering the working characteristics of high-speed permanent magnet machines, this paper analyzes the iron loss of HSPMM, in which the magnetic harmonics, rotating magnetic field and thermal effects are considered. A built 30 kW, 45000 r/min HSPMM is used as the study example, in which the FEA is applied to validate the effectiveness of the proposed approach.

Comparative results with FEA reveal that the new model can accurately compute the iron loss of HSPMM. The maximum prediction errors of the total iron loss are 3.73%, 3.14% and 3.05% respectively for 40℃, 100℃ and 150 ℃ temperature conditions, while the absolute average errors are all less than 3.03% regardless of the temperatures. Compared with the solutions via Bertotti model, the iron loss computation accuracy increases by around 25%. All the outcomes achieved in this paper can provide valuable references for the design and optimization of HSPMMs. The proposed method can also be extended to other types of electromagnetic devices like superconducting electrical machines.

REFERENCES

[1] A. Tenconi, S. Vaschetto, and A. Vigliani, "Electrical machines for high-speed applications: design considerations and tradeoffs," *IEEE Trans. Ind. Electron.*, vol. 61, no. 6, pp. 3022-3029, Jun. 2014.

[2] D. Gerada, A. Mebarki, N. L. Brown, C. Gerada, and A. Cavagnino, "High-speed electrical machines: technologies, trends, and developments," *IEEE Trans. Ind. Electron.*, vol. 61, no. 6, pp. 2946-2959, Jun. 2014.

[3] K. Muranaka, T. Nakamura, S. Okajima, T. Ogasa, N. Amemiya, and Y. Itoh, "Experimental and analytical studies on variable speed control of high-temperature superconducting induction/synchronous motor," *IEEE Trans. Appl. Supercon.*, vol. 26, no. 4, pp. 1-5, Jun. 2016.

[4] W. Qu, Z. Guo, Z. Mu, Y. Xing, and R. Liang, "Research on mechanical characteristics of high-speed permanent magnet motor," in *Proc. 2020 IEEE Int. Conf. on Applied Superconductivity and Electromagnetic Devices (ASEMD)*, Tianjin, 2020, pp. 1-2.

[5] N. Bianchi, S. Bolognani, and F. Luise, "Potentials and limits of high-speed PM motors," *IEEE Trans. Ind. Appl.*, vol. 40, no. 6, pp. 1570-1578, Nov.-Dec. 2004.

[6] Z. Kolondzovski, A. Arkkio, and J. Larjola, "Power limits of high-speed permanent-magnet electrical machines for compressor applications," *IEEE Trans. Energy Convers.*, vol. 26, no. 1, pp. 73-82, Mar. 2011.

[7] G. Du, W. Xu, J. Zhu, and N. Huang, "Effects of design parameters on the multiphysics performance of high-speed permanent magnet machines," *IEEE Trans. Ind. Electron.*, vol. 67, no. 5, pp. 3472-3483, May 2020.

[8] G. Du, W. Xu, J. Zhu, and N. Huang, "Power loss and thermal analysis for high-power high-speed permanent magnet machines," *IEEE Trans. Ind. Electron.*, vol. 67, no. 4, pp. 2722-2733, Apr. 2020.

[9] Y. Zhang, S. McLoone, W. Cao, and F. Qiu, "Power loss and thermal analysis of a MW high-speed permanent magnet synchronous machine," *IEEE Trans. Energy Convers.*, vol. 32, no. 4, pp. 1468-1478, Dec. 2017.

[10] A. S. Thomas, Z. Q. Zhu, and G. W. Jewell, "Proximity loss study in high speed flux-switching permanent magnet machine," *IEEE Trans. Magn.*, vol. 45, no. 10, pp. 4748-4751, Oct. 2009.

[11] Y. Zhang, S. McLoone, and W. Cao, "Electromagnetic loss modeling and demagnetization analysis for high speed permanent magnet machine," *IEEE Trans. Magn.*, vol. 54, no. 3, pp. 1-5, Mar. 2018.

[12] A. R. Tariq, C. E. Nino-Baron, and E. G. Strangas, "Iron and magnet losses and torque calculation of interior permanent magnet synchronous machines using magnetic equivalent circuit," *IEEE Trans. Magn.*, vol. 46, no. 12, pp. 4073-4080, Dec. 2010.

[13] H. W. Derbas, J. M. Williams, A. C. Koenig, and S. D. Pekarek, "A comparison of nodal- and mesh-based magnetic equivalent circuit models," *IEEE Trans. Energy Convers.*, vol. 24, no. 2, pp. 388-396, Jun. 2009.

[14] G. Lei, J. Zhu, and Y. Guo, *Multidisciplinary Design Optimization Methods for Electrical Machines and Drive Systems*, Berlin, Heidelberg: Springer Berlin / Heidelberg, 2016.

[15] G. Liu, M. Liu, Y. Zhang, H. Wang, and C. Gerada, "High-speed permanent magnet synchronous motor iron loss calculation method considering multiphysics factors," *IEEE Trans. Ind. Electron.*, vol. 67, no. 7, pp. 5360-5368, Jul. 2020.

[16] J. Seo, T. Chung, C. Lee, S. Jung, and H. Jung, "Harmonic iron loss analysis of electrical machines for high-speed operation considering driving condition," *IEEE Trans. Magn.*, vol. 45, no. 10, pp. 4656-4659, Oct. 2009.